Gold nanorods vs. gold nanoparticles: Application in electrochemical sensing of cytosine β-D-arabinoside using metal ion mediated molecularly imprinted polymer

Bhim Bali Prasad*, Ragini Singh and Anil Kumar

Analytical Division, Department of Chemistry, Faculty of Science, Banaras Hindu University, Varanasi-221005, India

** Corresponding author. E-mail address: prof.bbpd@yahoo.com Phone +91 9451954449; Fax: +91 542 2268127*

Electronic Supplementary Information (ESI):

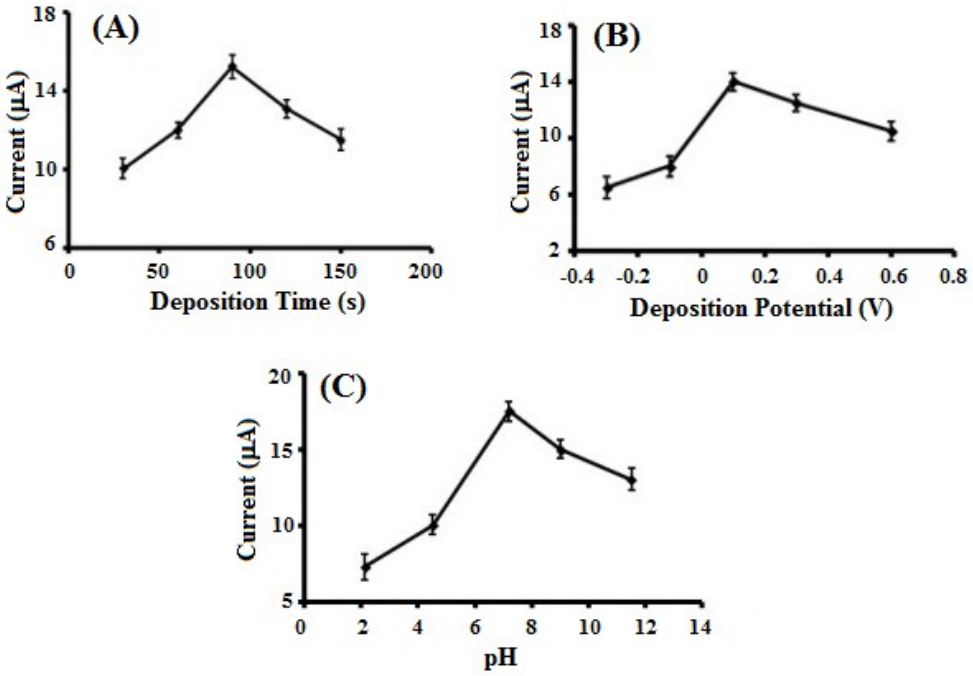

Fig. S1 Optimization of analytical parameters: (A) deposition potential, (B) deposition time, and (C) pH.

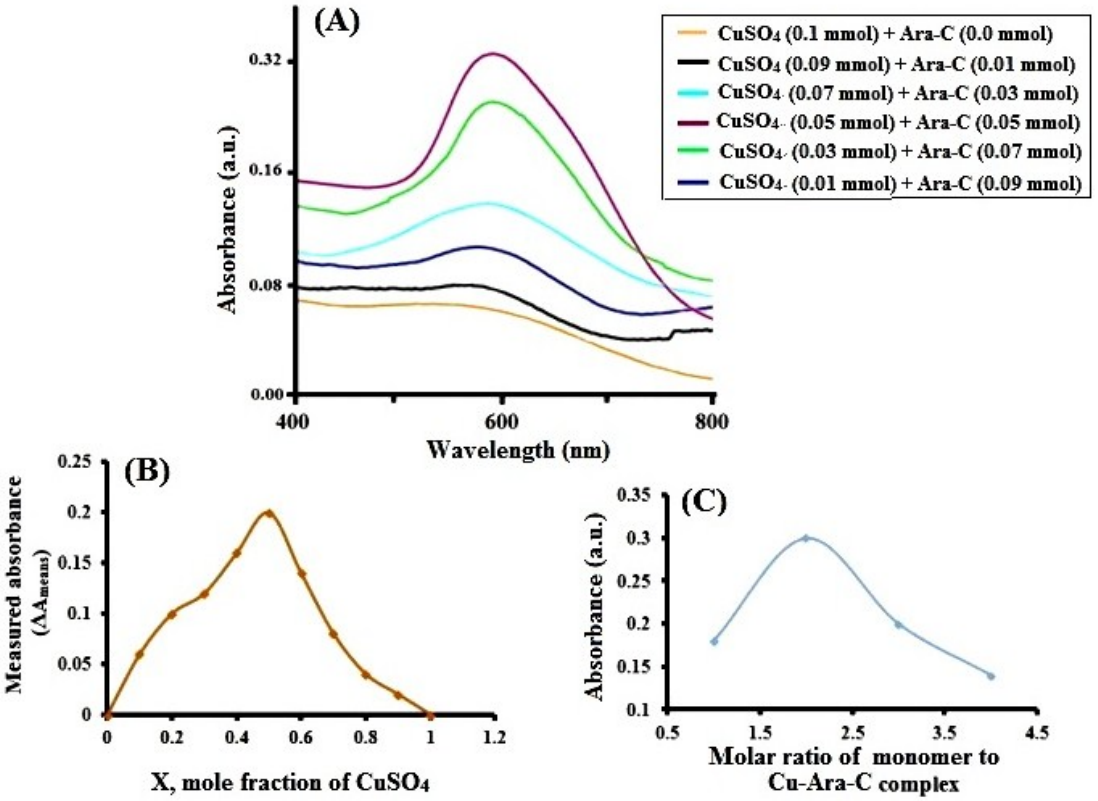

Fig. S2 (A) UV-visible spectra of $CuSO_4$ for various concentrations of Ara-C, (B) Job's plot for $CuSO_4$-Ara-C complex, at 600 nm, and (C) complexometric titration of Cu(II)-Ara-C with various concentrations of monomer (MAC) at 620 nm.

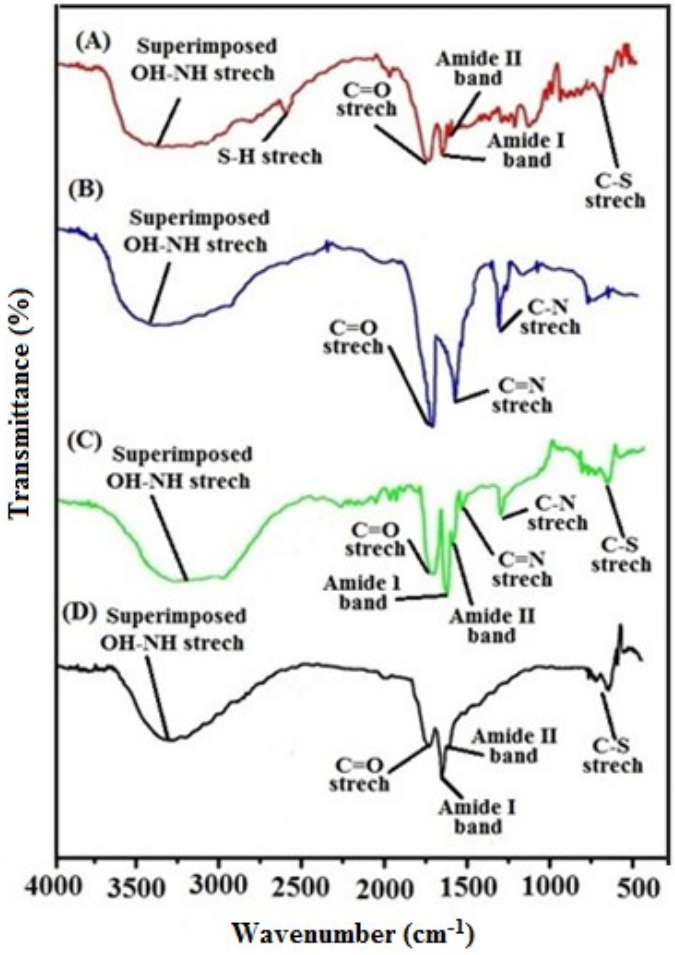

Fig. S3 FT-IR (KBr) spectra of monomer (A), template (B), CIP-adduct (C), and CIP (D).

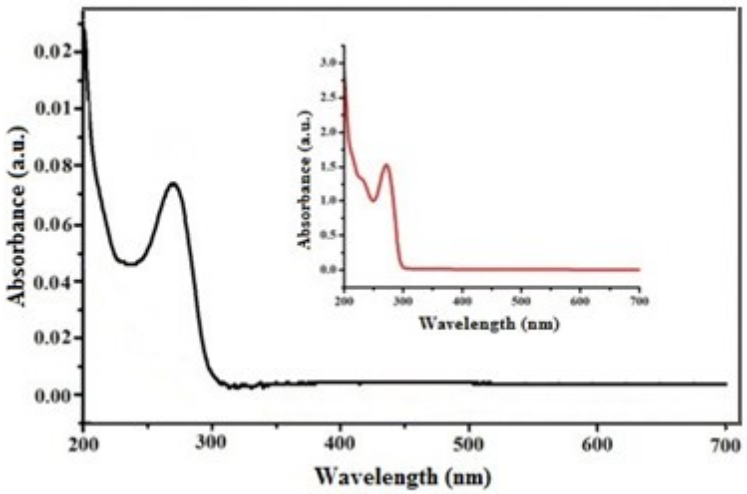

Fig. S4 UV-vis spectrum of the HCl extract of Ara-C (inset shows UV-vis spectrum of standard Ara-C solution in HCl).

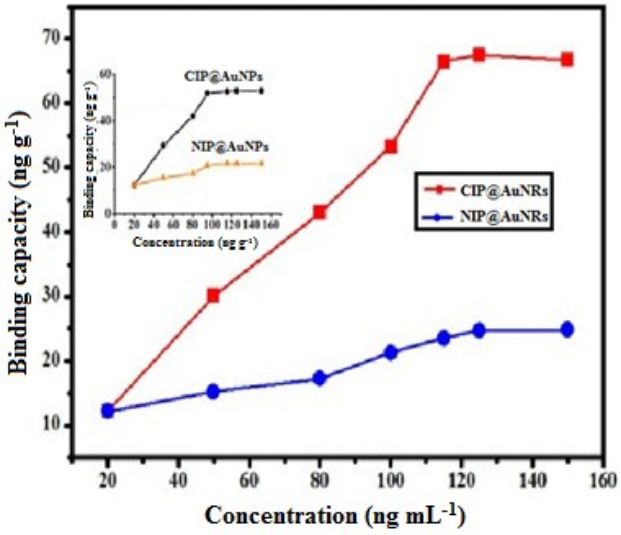

Fig. S5 Binding affinity of CIP/NIP@AuNRs toward Ara-C. Inset shows binding affinity of CIP/NIP@AuNPs toward Ara-C .

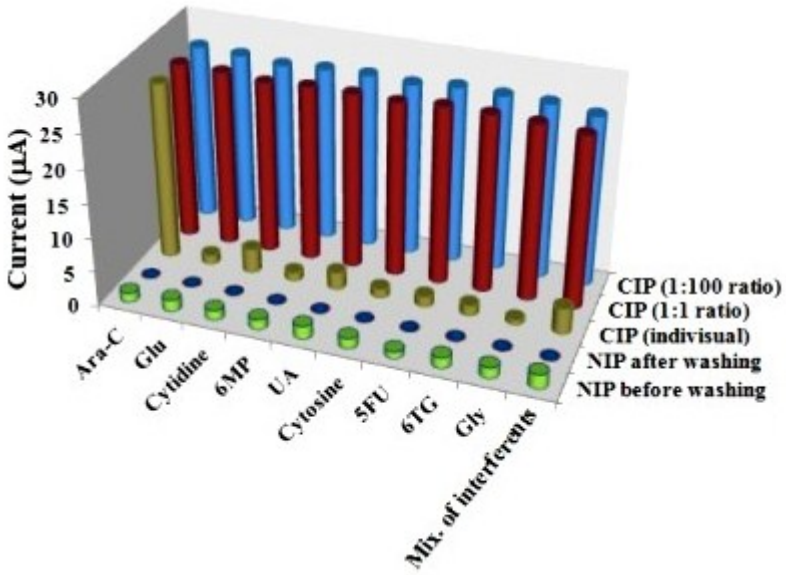

Fig. S6 Recognition selectivity and cross reactivity on CIP@AuNRs/PGE and NIP@AuNRs/PGE.

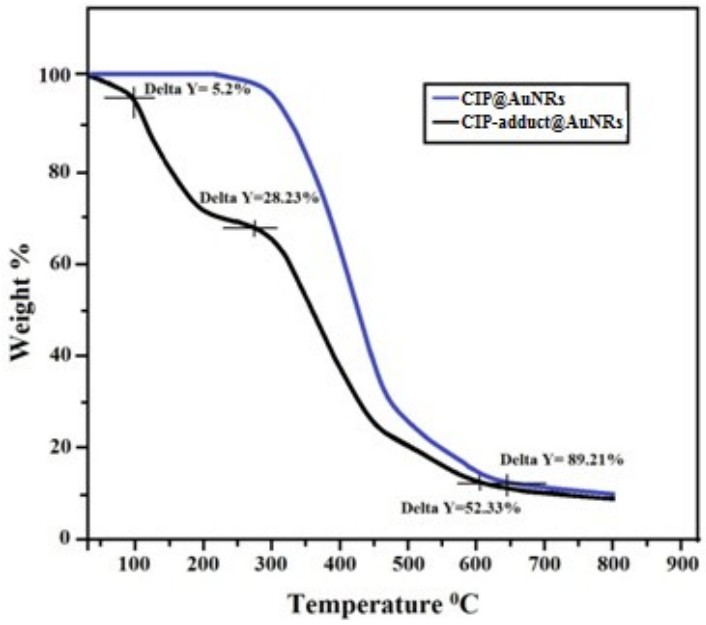

Fig. S7 TGA of CIP@AuNRs and CIP-adduct@AuNRs composites.

Table S1 Comparison of different methods of Ara-C determination

S.N.	Method	*LODs* (ng mL^{-1})	Range (ng mL^{-1})	Recovery (%)	Remarks	Ref.
1.	Direct electrochemical detection at mercury electrode	97.28	7.3×10^2 - 97.3×10^3	-	No analysis in real samples, no interference studies	[1]
2.	HPLC-UV detection	20.0	3.2×10^2 - 10.0×10^3	-	No analysis in real samples, no interference studies	[2]
3.	RP-HPLC-UV detection	150.0	25.0×10^3 - 150×10^3	100.4 - 100.8	No analysis in real samples, no interference studies	[3]
4.	Flow injection analysis based chemiluminescence system	0.18	1.45 - 24.30	-	No analysis in real samples	[4]
5.	RP-HPLC	-	2.0×10^3 - 15.0×10^3	98.1 - 98.7	No analysis in real samples, no interference studies	[5]
6.	HPLC-UV detection	2.0	50 - 20×10^3	98.3 - 103.2	No analysis in urine sample	[6]
7.	HPLC-MS detection	-	0.5 - 500.0	-	No analysis in urine sample	[7]
8.	CIP@AuNRs/PGE	0.19	1.0 - 126.7	97.0 - 100.0	Very low *LODs*, trace analysis in, serum ,urine and pharmaceutical	Present work

S1. Optimization of accumulation potential, time and pH

For DPASV measurement, various parameters, viz., deposition potential (E_{acc}), deposition time (t_{acc}) and pH, have been optimized (Fig. S1). Accordingly, the DPASV peak height for Ara-C (45.0 ng mL^{-1}) increased with the increase of t_{acc} up to 90 s and then decreased. The diminishing trend is due to the saturation of molecular cavities by Ara-C molecules. The effect of E_{acc} on the DPASV peak current (I_p) was also examined, in the potential range varying from -0.3 to 0.6 V. Accordingly, the maximum development of I_p was reached at 0.1 V; any potential more negative than 0.1V revealed an instant decrease in DPASV response owing to electrostatic repulsion between electron-rich Ara-C moiety and negatively charged electrode. The diminishing current response at potential more +ve than 0.1 V may reflect binding sites saturation. Further, the study on the effect of solution pH revealed a gradual rise in current attaining maximum at pH 7.2. At lower pH, the H^+ ion can compete with Cu^{2+} ion for ligand in the solution. However, at >7.2, the decreasing trend of response may be associated with instability of "complex-template".

S2. Stoichiometry

As a proof of concept regarding the role of metal ion toward imprinting process, the stability constant (β) of metal- Ara-C complex, was calculated following an empirical equation[8]:

$$\frac{1}{i_p} = \frac{1}{i_{p\,max}} + \frac{1}{i_{p\,max}\beta C_t^m} \qquad (1)$$

where i_p is the measured peak current, $i_{p\,max}$ the peak current when all template molecules formed complex with CIP cavity, C_t is the concentration of template, m is the coordination number of the complex formed between template and metal ion. By plotting $1/i_p$ *vs.* $1/C_t^m$ for different 'm' values, a straight line will be obtained. In our work, when m = 1, a perfect straight line with R^2 = 0.99 was obtained, indicating 1:1 complexation between Cu^{+2} and Ara-C with stability constant (β = 0.194). In the metal ion mediated imprinting, the exclusive role of metal ion is to act as mediator for the polymerization of template-metal ion-monomer self assembled complex. The β values with other mediating ions, viz., Ni^{+2} and Zn^{+2} were calculated as 0.035 and 0.051, respectively.

S3. Polymeric characteristic

The recognition ability of imprinted polymer is primarily dependent on both the print molecule and functional precursors of the monomer. The optimum amount of cross-linker in CIP synthesis not only fixes the binding cavities but also imparts requisite stability to

polymer network with development of adequate pores for analyte access. This was explored by the maximum development of DPASV peak current when cross-linker amount increased up to 1.0 mmol. The gradual decreasing current above this amount of cross-linker could be apparently due to the higher degree of cross-linkages and thereby restricted analyte uptake. Polymerization time and polymerization temperature are the other influencing parameters governing the polymer porosity. Lower polymerization (<3 h) time responded lower current due to inadequate number of binding sites. However, longer polymerization time (>3 h) might have led an extensive cross-linking and restricted porosity that resulted in lower current response. Thus, a polymerization time of 3 h was found to be optimum for a better current response. Insofar as polymerization temperature is concerned, 70 ^{0}C was found appropriate to respond optimum current; any temperature below this may cause sluggish polymerization and take longer time.

S4. Langmuir Binding isotherm

Selective adsorption of analyte from bulk to CIP cavities for CIP@AuNRs/PGE can be explained using the Langmuir equation [9]:

$$\theta = \frac{bc}{1 + bc} \tag{2}$$

where θ is the ratio of the surface coverage 'Γ^0' at any analyte concentration 'C' to its maximum surface coverage Γ^{max}. Eq. (2) can be rearranged as,

$$\frac{C}{\Gamma^0} = \frac{1}{b\Gamma^{max}} + \frac{C}{\Gamma^{max}} \tag{3}$$

Accordingly, a linear equation C/Γ^0= (924.3387 ± 86.6692)×10^6 C + (153.2033 ± 4.9467) (R^2 = 0.98) representing C/Γ^0 vs. C plot is obtained. The perfect linearity reflects uniform binding sites in CIP motif. The intercept (equivalent to slope/b) of above equation revealed adsorption coefficient (b) to be 6.03×10^6 L mol^{-1}. The Gibbs free energy change ($\Delta G = -RT\ ln\ b$) due to analyte adsorption could be calculated as -38.68 kJ mol^{-1} which indicates analyte adsorption to be a spontaneous process.

S5. Chronocoulometry

Peak potential of an ir-reversible process obeys the following equations.[10]

$$E_p - E_{p/2} = \frac{47.7}{\alpha} \tag{4}$$

$$\alpha n = \frac{1.857RT}{F\left[E_p - E_{p/2}\right]} \quad (5)$$

where α = transfer coefficient, E_{pa} = peak potential, $E_{pa/2}$ = half peak potential, and n = number of electron participated in reaction; other parameters have their usual meanings. Based on these equations, α and n values were calculated as 0.681 and 1.0 respectively. The fractional α value suggests irreversible oxidation of analyte.

Chronocoulometric measurements were also performed for the calculation of surface coverage (Γ^0) and diffusion coefficient (D) of the analyte. According to the integrated Cottrell equation[10], the relationship between charge (Q) vs. square root of time ($t^{1/2}$) can be described as follows:

$$Q = 2nFACD^{1/2}_t\pi^{-1/2} + Q_{ads} + Q_{dl} \quad (6)$$

$$Q_{ads} = nFA\Gamma^0 \quad (7)$$

where A is electrochemical surface area of electrode (24.65×10^{-2} cm^2), C is the concentration (41.0 nmol L^{-1}) of Ara-C, Q_{dl} is the double layer charge, Q_{ads} is the Faradaic oxidative charge; and other symbols have their usual meaning. For CIP@AuNPs and CIP@AuNRs modified PGEs, Q_{dl} and total charge (Q_{dl} +Q_{ads}) were estimated from the respective intercepts of the Anson plots (Q vs. $t^{1/2}$) in the absence and presence of Ara-C. Accordingly, Γ^0 was calculated to be 1.66×10^{-11} and 2.12×10^{-10} mol cm^{-2} for CIP@AuNPs and CIP@AuNRs modified PGEs, respectively. It is interesting to note that in the case of CIP, Γ^0 approximates surface coverage of analyte molecules which are specifically bound to CIP cavities. Therefore, total electrode surface was covered by 2.44×10^{-12} mol (1.47×10^{12} molecule) and 5.23×10^{-11} mol (3.15×10^{13} molecule) of Ara-C, i.e. equivalent to 1.47×10^{12} and 3.15×10^{13} cavities (each molecule per cavity) for CIP@AuNPs and CIP@AuNRs modified PGEs, respectively. This revealed greater number of cavities on CIP@AuNRs/PGE electrode than CIP@AuNPs/PGE. From the slope of the Anson plot 'D' values calculated for Ara-C were found to be 1.5×10^{-5} and 5.29×10^{-4} cm^2 s^{-1} for CIP@AuNPs and CIP@AuNRs modified PGEs, respectively. The higher 'D' values may be attributed to the unhindered diffusivity of the template in between the pores of vertically tethered bristles of CIP@AuNRs composite.

In order to comprehend the electron-transfer kinetics at CIP@AuNPs/PGE and CIP@AuNRs/PGE, we have calculated the standard heterogeneous rate constant (k) for both electrodes using Velasco equation[11]:

$$k = 1.11D^{1/2}\left(E_p - E_{p/2}\right)^{-1/2}v^{1/2} \quad (8)$$

The estimated k values at CIP@AuNPs/PGE and CIP@AuNRs/PGE are found to be 1.75×10^{-3} and 1.36×10^{-2} cm s^{-1}, respectively. The higher k value for Ara-C indicates that the oxidation of Ara-C is faster at the CIP@AuNRs/PGE than the CIP@AuNPs/PGE.

S6. Batch binding

To investigate the binding affinity of Ara-C with CIP and NIP-based AuNPs and AuNRs/PGEs, equilibrium batch binding experiments were performed (Fig. S5, ESI†) using UV-vis spectrometry. Optimum adsorption capacities (Q) were found to be 66.5 and 24.8 ng g^{-1} analyte on CIP@AuNRs and NIP@AuNRs, respectively. The maximum value of adsorption capacities on CIP@AuNPs and NIP@AuNPs were found to be 52.7 and 21.5 ng g^{-1}, respectively. The NIP@AuNRs/AuNPs showed relatively a low binding affinity toward Ara-C due to lack of recognition sites. The meagre adsorption observed with NIP-based electrode could be termed as non-specific contributions.

S7. TGA analysis

As evinced from TGA curves, CIP degradation (Fig. S7) proceeds with the gradual weight loss in the temperature range: 275-650 ^{0}C, corresponding to the weight loss of 89.2%. This degradation may tentatively be assigned due to Cu^{+2}-monomer degradation. On the other hand, CIP-adduct showed three weight losses: 35.2-100 ^{0}C, 100-275.3 ^{0}C and 275.3-607.5 ^{0}C corresponding to 5.2% (water moisture), 28.2% (template) and 52.3% (Cu^{+2} -monomer) degradations, respectively. The observed weight loss of in second step of TGA curve of CIP-adduct corroborates the calculated loss (29.4%) due to the template degradation from the polymer motif. Since there was no weight loss observed in TGA curve of CIP, one may conclude the complete retrieval of template molecules from CIP-adduct motif.

References:

1 D. Marin and C. Teijeiro, *Bioelectrochem.Bioenerg.*, 1992, **28**, 417-424.

2 A. F. Mistiran, A. A. Dzarr, and S. H. Gan, *Toxicol. Mech. Meth.*, 2010, **20(8)**, 472–481.

3 A. Bhatnagar, S. Loura and M. Chaudhary, *Eurasian J Anal. Chem.*, 2012, **7(3)**, 160-167.

4 Z. Cai, X. Zhang, D. F. Lu, and J. N. Gan, *Bull. Korean Chem. Soc.,* 2012, **33**, No. 1, 171.

5 S.N. Murthy, A. Rohini, K.E. Pravallika, A. Prameela Rani and S.A. Rahaman, *IJSPR* 2013, **4(12)**, 4573-4576.

6 L. Yuandong, L. Ningsheng, W. Jingsong, L. Yi, *China pharmacy*, 2006, 17.

7 M. J. Hilhorst, G. Hendriks, M. WJ van Hout, H. Sillén and N. C. Merbel, *Future Science*, 2011, **3**, 1603-1611.

8 Gao, X., 1986. *Handbook on the Physics and Chemistry of Rare Earths* **8**, 163-201.

9 M.F. Smiechowski, V.F. Lvovich, S.Roy, A. Fleischman, W.H. Fissell, A.T. Riga, *Biosens.Bioelectron.*, 2006, **22**, 670–677.

10 A.J. Bard, L.R. Faulkner, Electrochemical Methods: Fundamental and Applications, 2nd ed., *Willey*, New York, 2001.

11 J.G. Velasco, *Electroanalysis*, 1997, **9**, 880.